STUDIES ON THE SEEPAGE VELOCITY UNDER THE DAM ON THE PERVIOUS FOUNDATION OF INFINITE THICKNESS

By Fumiya Yahagi, C.E. Member*

1. Introduction

The dam resting on the pervious strata must be designed so as the underseepage velocity may not exceed the limited value for the breakdown of the foundation.

The underseepage flow has been both theoretically and experimentally studied by many investigators for a long time. An actual dam, however, has been designed by the "creep ratio", advocated before half century by Bligh and Griffith and thereafter revised by E.W. Lane[1]. But it is only a conventional procedure, and has no theoretical relation to the physical character of the dam foundation. Recently Awazu[2] criticized the creep theory and tried to revise it, from the view point that the piping phenomenon breaks out when the mean hydraulic gradient in the flow flux, surrounded by the surface of the structure and a certain group of streamlines in the foundation, becomes more than a certain value.

The purpose of the present paper is the discussion of the seepage velocity under a dam on the pervious strata of infinite thickness, as well as criticizing the creep theory, and its application to the more theoretical design of a floating dam secured from underseepage, based on the theoretical derivation of the seepage velocity at an arbitrary point under a dam.

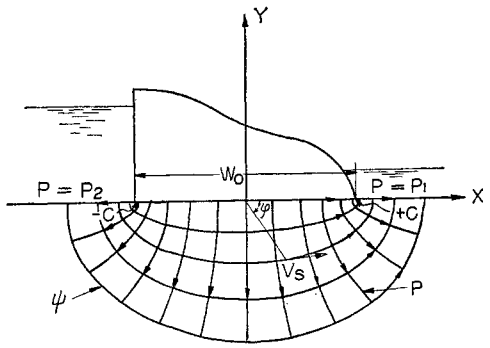

Fig. 1 Underseepage flow of a dam resting on a pervious foundation of an infinite thichness.

* Technical Laboratory Rentral Sesearch Institute of Electric Power Industry

This paper is the abbreviation of the monograph[3] in Technical Laboratory, Central Research Institute of Electric Power Industry.

2. Seepage velocity under a dam on an isotropic pervious foundation of infinite thickness

In the case of the dam, of which the width is 2c and its length is very longer than its width, resting on an isotropic pervious fonndation of infinite thickness, as in Fig. 1, the flow system is represented by the following conjugate function:

$$\left.\begin{aligned} f(z)=\psi+ip&=\cosh^{-1}\frac{x+iy}{c},\\ \phi&=\frac{k}{\mu}p \end{aligned}\right\}\quad\cdots\cdots(1)$$

ϕ being the velocity potential, p, fluid pressure, k, coefficient of permeability, μ, fluid viscosity, and ψ, stream function.

The pressure and streamline distribution are then given explicitly by

$$\left.\begin{aligned} p&=\cos^{-1}H,\\ \psi&=\cosh^{-1}H, \end{aligned}\right\}\quad\cdots\cdots(2)$$

where

$$H=\left[\frac{(x^2+y^2+c^2)^2\pm\sqrt{(x^2+y^2+c^2)^2-4x^2c^2}}{2c^2}\right]^{1/2}\quad\cdots\cdots(3)$$

the plus sign referring to ψ and the minus one to p. The tangential velocity v_s along a streamline is given by

$$v_s=-\operatorname{grad}\phi=-\frac{k}{\mu}\frac{dp}{ds}.$$

Then, through these equations,

$$v_s=\frac{k\,\Delta p}{\mu}\times\frac{e}{c\pi}\sqrt{\frac{1-e^2\cos^2\varphi}{1-e^2(2-e^2)\cos^2\varphi}}\quad\cdots(4)$$

can be obtained. If the difference between the head and the tail water level is denoted by ΔH, and the effective permeability $\bar{k}$, v_s is rewritten by

$$\left.\begin{aligned} v_s&=\frac{\bar{k}\,\Delta H}{w_0}\times B,\\ B&=\frac{2e}{\pi}\sqrt{\frac{1-e^2\cos^2\varphi}{1-e^2(2-e^2)\cos^2\varphi}}. \end{aligned}\right\}\quad\cdots\cdots(5)$$

Eq. (5) shows the seepage velocity at an arbitrary point along an arbitrary streamline ψ_0

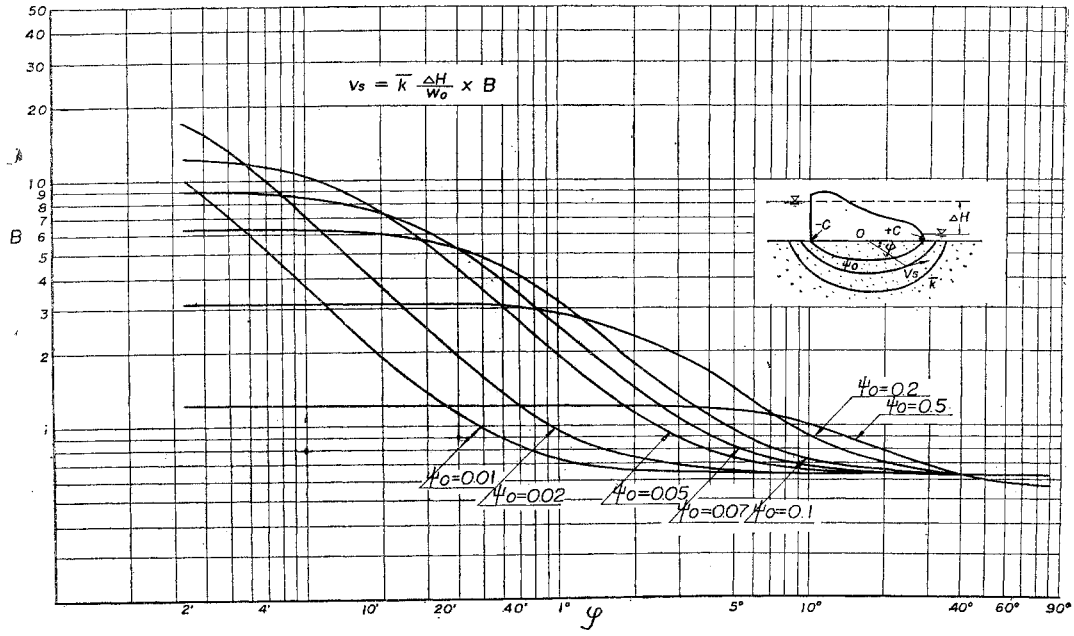

Fig. 2 Variation of the velocity coefficient B with center angle φ.

$=\cosh^{-1}(1/e)$ under a dam of width w_0, where B is called the "velocity coefficient" in the case of no sheet piling. Fig. 2 shows the variation of B with φ, and shows that the seepage velocity is minimum at the point just under the dam center ($\varphi=-\pi/2$) and tends to become larger towards the ends until it becomes maximum at the extremities ($\varphi=0, -\pi$), where the flow seeps into and out of the foundation. When the velocity coefficient and the velocity itself at these extremities are denoted by B_0 and v_{s0} respectively, they are given from Eq. (5) in the following,

$$\left.\begin{aligned} v_{s0} &= \frac{\bar{k}\,\Delta H}{w_0} \times B_0, \\ B_0 &= \frac{2e}{\pi\sqrt{1-e^2}} \end{aligned}\right\} \quad \cdots\cdots(6)$$

It is shown that if $e=1$, *i.e.*, at the heel or toe of the dam, the velocity leads to infinity[4]. The value of B_0 is illustrated in Diagram 1.

Although the above result is based on the approximation that the foundation is infinitely thick, this approximation will not involve serious errors when the base width w_0 is less than the foundation thickness h, because there is only inappreciable difference between the pressure distribution along the base in the case of $h>w$ and the one in the case of $h=\infty$.

In the case of the dam with sheet piling in

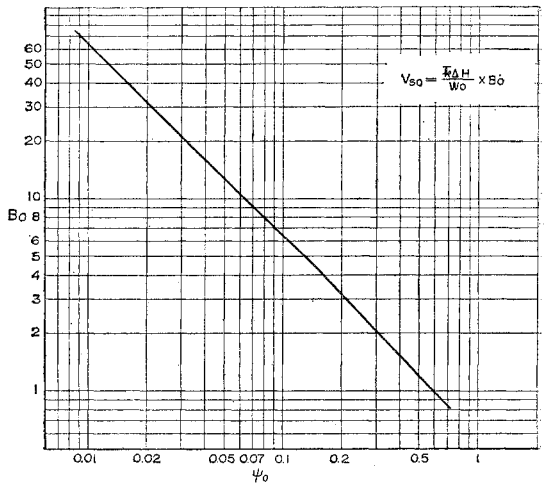

Diagram 1 B_0-diagram.

a single line, z-plane representation is transformed to ζ-plane, where the dam with sheet piling in z-plane is reduced to the one with no sheet piling, by

$$z=-d_0\sqrt{\zeta^2-1}+b \quad \cdots\cdots(7)$$

by Schwarz-Christoffel theorem, d_0 being the piling depth and b, the distance of piling from the dam center. The equations representing a streamline are given by Eq. (7) as follows:

$$\left.\begin{aligned} x-b &= \pm\frac{d_0}{\sqrt{2}}\sqrt{\sqrt{(\xi^2-\eta^2-1)^2+4\xi^2\eta^2}+(\xi^2-\eta^2-1)}, \\ y &= \frac{d_0}{\sqrt{2}}\sqrt{\sqrt{(\xi^2-\eta^2-1)^2+4\xi^2\eta^2}-(\xi^2-\eta^2-1)}. \end{aligned}\right\} \quad \cdots\cdots(8)$$

The seepage velocity v_s along the streamline $\psi=\psi_0$ is analysed through some treatments as* follows:

$$\left.\begin{aligned}
&\frac{\xi'^2}{\cosh^2\psi_0}+\frac{\eta'^2}{\sinh^2\psi_0}=1, \qquad \xi=N\xi'+M, \qquad \eta=N\eta' \\
&M=\frac{1}{2}\left[\sqrt{1+\frac{\left(\frac{1}{2}-\frac{b}{w_0}\right)^2}{\left(\frac{d_0}{w_0}\right)^2}}-\sqrt{1+\frac{\left(\frac{1}{2}+\frac{b}{w_0}\right)^2}{\left(\frac{d_0}{w_0}\right)^2}}\right]; \qquad N=\frac{1}{2}\left[\sqrt{1+\frac{\left(\frac{1}{2}-\frac{b}{w_0}\right)^2}{\left(\frac{d_0}{w_0}\right)^2}}+\sqrt{1+\frac{\left(\frac{1}{2}+\frac{b}{w_0}\right)^2}{\left(\frac{d_0}{w_0}\right)^2}}\right]; \\
&v_s=\frac{\bar{k}\,\Delta H}{w_0}\times D \\
&D=\frac{1}{\left(\frac{d_0}{w_0}\right)\pi}\times\frac{\sqrt{1-e^2}\,\sqrt[4]{\{(\xi^2-\eta^2-1)^2+4\,\xi^2\eta^2\}^3}}{\sqrt{\{\eta^2(\xi^2+\eta^2+1)+(1-e^2)\xi(\xi-M)(\xi^2+\eta^2-1)\}^2+\eta^2\{\xi(\xi^2+\eta^2-1)-(1-e^2)(\xi-M)(\xi^2+\eta^2+1)\}^2}} \\
&e=\frac{1}{\cosh\psi_0}
\end{aligned}\right\} \qquad \cdots\cdots(9)$$

D is the velocity coefficient in the case of sheet piling present. Fig. 3 is an example of illustrations of D which show the velocity distribution along the streamline $\psi_0=0.01$, evaluated from Eq. (8) in the case of sheet piling of depth d_0

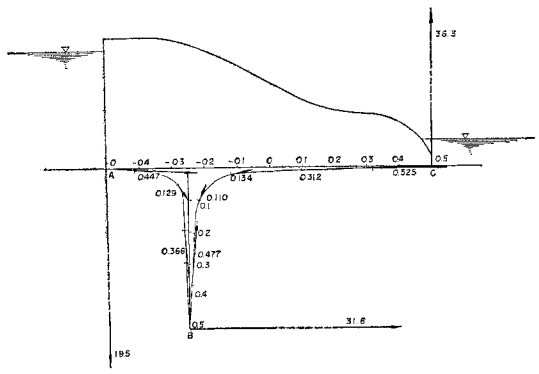

Fig. 3 An example of the velocity distribution under a dam with sheet piling. Sheet piling is at the middle of the upstream half of the dam, its depth equals to half of the base width, and the stremline is $\psi_0=0.01$.

Vectors and figures show the magnitude and the direction of the velocities at respective points.

$=w_0/2$ present at a quarter of the base width from the heel. As will be readily seen from this illustration and others, the velocity becomes maximum generally at seeping-in and -out points and the extremity of sheet piling. On the contrary, in concave parts of the streamline, it becomes small, the minimum being far less than 1/100 of the maximum in such a case as $\psi_0=0.01$, which will cause the possible occurence of the dead water zone in such parts. Those maximum velocities may play an important role in the security of a floating dam. If the velocity and its coefficient at the seeping-in or-out points are denoted by v_{s0} and D_0 respectively, v_{s0} is given by, through Eq. (9)

$$\left.\begin{aligned}
&v_{s0}=\frac{\bar{k}\,\Delta H}{w_0}\times D_0 \\
&D_0=\frac{1}{\left(\frac{d_0}{w_0}\right)\pi}\times\frac{\xi^2-1}{(1-e^2)\xi(\xi-M)} \\
&e=\frac{1}{\cosh\psi_0}
\end{aligned}\right\} \qquad \cdots\cdots(10)$$

Diagrams 2 show the variation of D_0 with d_0/w_0 in the various streamlines. D_{in} represents

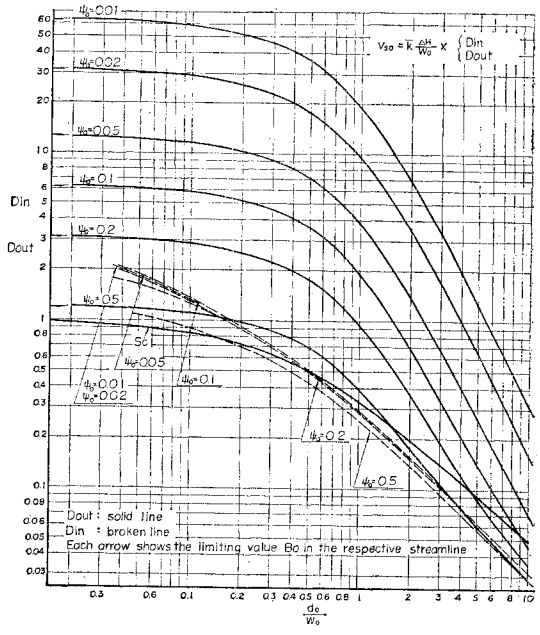

Diagram 2 D_0-diagram

(a) when sheet piling is at the heel or the toe of the dam ($b=-c$ or c).

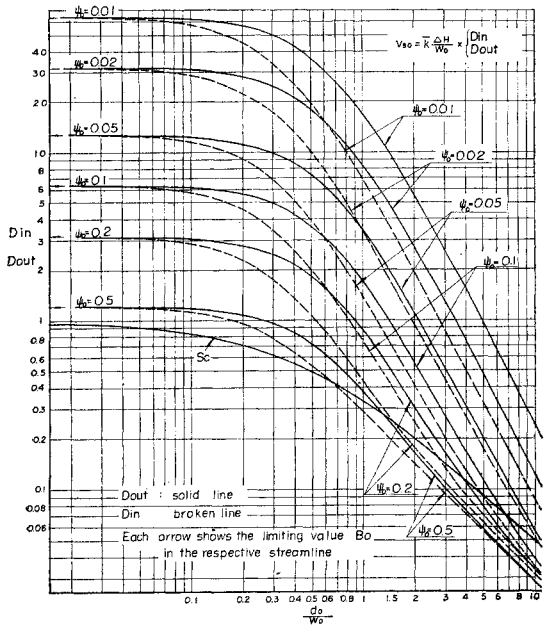

Diagram 2 d_0-diagram
(b) when sheet piling is at the middle of the upstream or down-stream half of the dam ($b=-c/2$ or $c/2$).

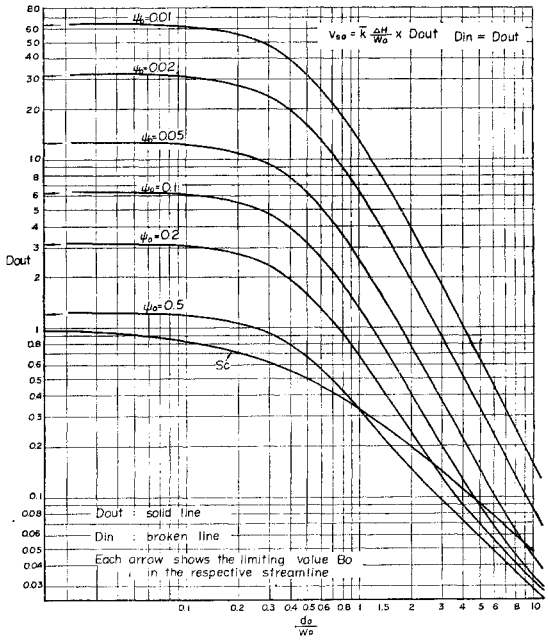

Diagram 2 d_0-diagram
(c) when sheet piling is at the center of the dam ($b=0$).

D_0 for seeping-in velocity and D_{out}, for seeping-out one. Notations (a), (b), and (c) in the diagram correspond to sheet piling at the heel ($b=-c$), at a quarter of the base width from the heel ($b=-c/2$), and at the center of the base ($b=0$) respectively. As will be seen in these figures, the velocity becomes small as the streamline goes far off the structure and as d_0/w_0 increases. If sheet piling is in the up stream half of a dam, D_{out} is always greater than D_{in}. When it is at the heel, D_{in} for streamlines less than about $\psi_0=0.1$ remains almost constant.

In order to examine the effect of the depth or the position of sheet piling to the velocity very near the dam, it is necessary to compare them at the point equally distant from the structure. The constant distance l from the dam is fixed upon the distance in a case of $\psi_0=0.05$, $d_0/w_0=1$, and $b=0$, as an illustration. Fig. 4 shows these relative variations, the velocity in the case of no sheet piling being chosen as unit. The seeping-in velocity decreases more rapidly than the seeping-out one does, as the piling depth increases. The effect of the piling position is also greater in the former than in the latter. In order to reduce the seeping-out velocity by half, piling depth is needed to equalize the base width, and moreover, to reduce it to 1/10, it is necessary to make the piling depth 6

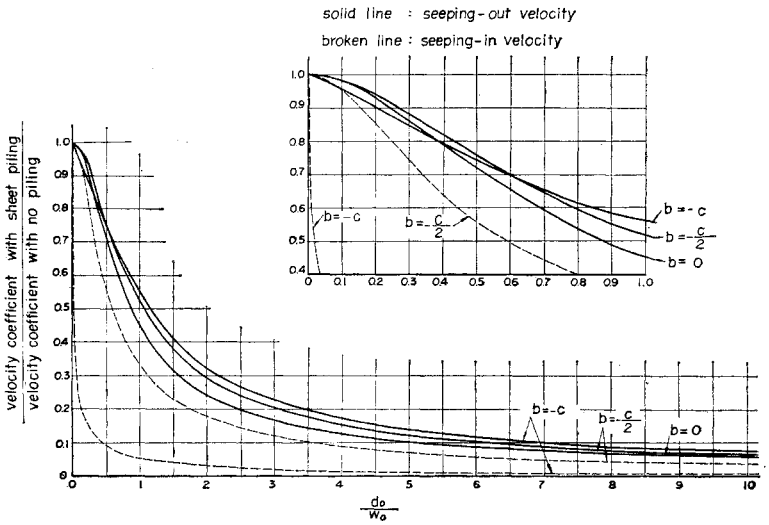

Fig. 4 Effect of piling depth and its position to seeping in and -out velocity.

times the base width. Generally the seeping-out velocity is almost inversely proportional to the piling depth if $d_0 < w_0$, but when $d_0 > w_0$, the velocity does not decrease so as the piling depth increases.

The effect of the position of sheet piling to the seeping-out velocity varies slightly with the piling depth, but it is fairly insignificant as a whole, and the maximum lessening of the velocity by the most effective position of sheet pil-*ing is at best about 10%.

Next, it is necessary to examine the seeping velocity around the extremity of sheet piling, where another maximum velocity arises. This maximum velocity v_{sp} along a certain streamline must arise at the point where the equipotential line originating from the extremity of sheet piling crosses the said streamline. Therefore, from Eq. (9), v_{sp} is given by

$$v_{sp}=\frac{\bar{k}\,\Delta H}{w_0}\times D_p$$

$$D_p=\frac{1}{\left(\frac{d_0}{w_0}\right)\pi}\times\frac{\sqrt{1-e^2}\sqrt[4]{\{(\xi_p^2-\eta_p^2-1)^2\{\eta_p^2+4\xi_p^2\eta_p^2\}^3}}{\sqrt{\{\eta_p^2(\xi_p^2+\eta_p^2+1)+(1-e^2)\xi_p(\xi_p-M)(\xi_p^2+\eta_p^2-1)\}^2+\eta_p^2\{\xi_p(\xi_p^2+\eta_p^2-1)^2-(1-e^2)(\xi_p-M)(\xi_p^2+\eta_p^2+1)\}^2}},$$

$$\xi_p=M\left(1-\frac{1}{e}\right),\qquad \eta_p=\sqrt{\left(\frac{1}{e^2}-1\right)(N^2-M^2)}\,,\qquad e=\frac{1}{\cosh\psi_0} \qquad \cdots\cdots(11)$$

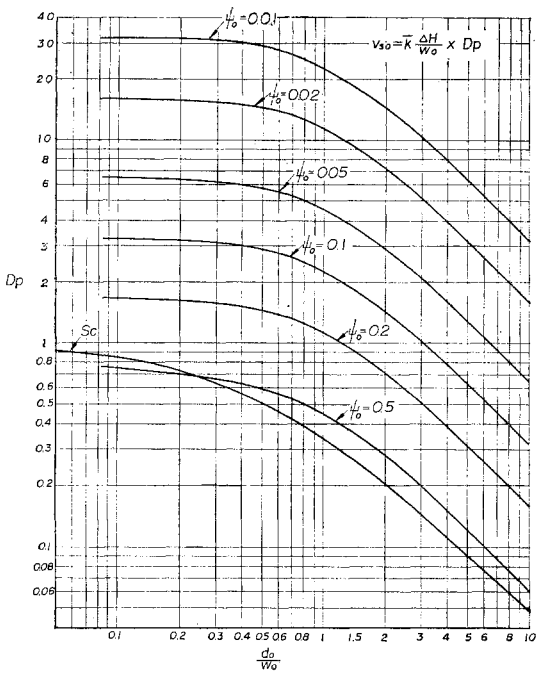

Diagram 3 D_p-diagram
(a) when sheet piling is at the heel or the toe of the dam ($b=-c$ or c).

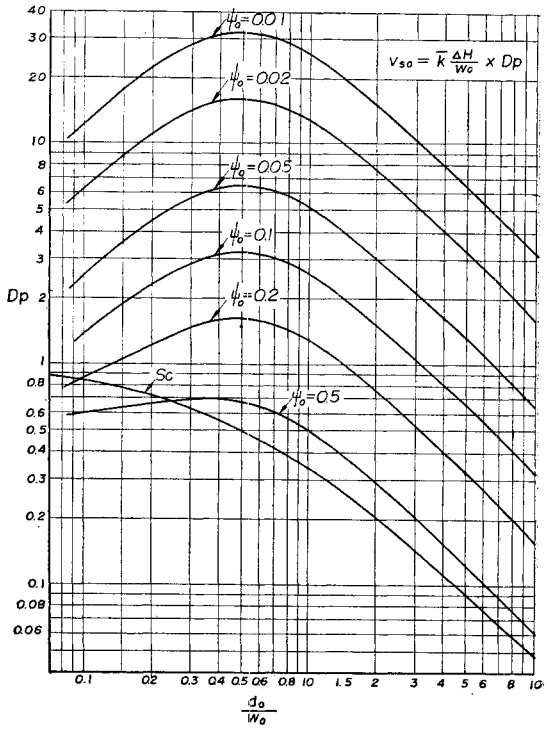

Diagram 3 D_p-diagram
(b) when sheet piling is at the middle of the upstream or downstream half of the dam ($b=-c/2$ or $c/2$),

D_p being the velocity coefficient at the maximum velocity point near the extremity of sheet piling. Diagrams 3 (a), (b), and (c) illustrate the variations of D_p with d_0/w_0 in various streamline. From these, the maximum velocity v_{sp} for a dam with sheet piling of any depth may be evaluated for these streamlines.

Fig. 5 shows the effect of the base width to v_{sp} at the point in always equal distance l from the extremity of sheet piling, l being the same distance as the previously described one. The

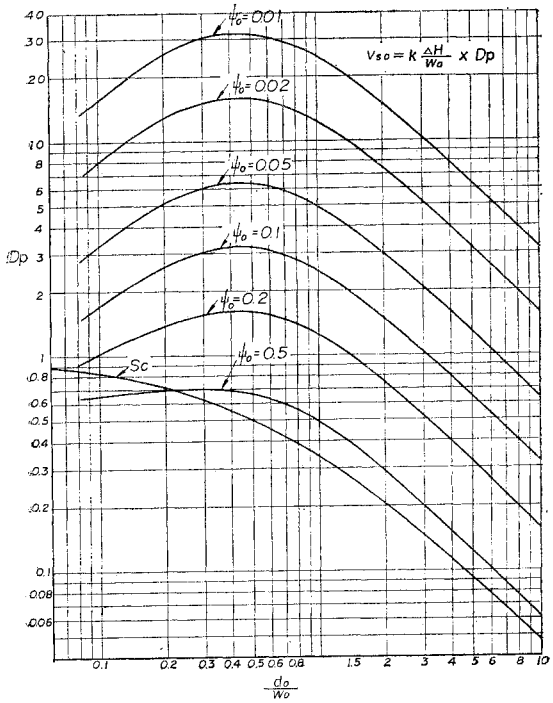

Diagram 3 D_p-diagram
(c) When sheet piling is at the center of the dam.

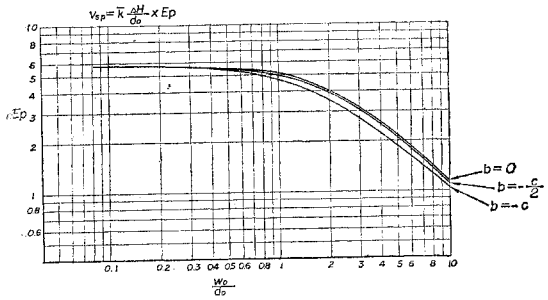

Fig. 5 Effect of the base width to the maximum velocity v_{sp} near the extremity of sheet piling.

maximum velocity remains almost constant during $w_0<d_0$, and it is after the base width exceeds the piling depth that the widening of the base contributes to lessen v_{sp}.

The seepage in a coffer dam can be examined as the extreme case as follows: The seeping-in and -out velocities, and the velocity around the extremity of the coffer dam are obtained from substituting $w_0=0$ in Eqs. (10) and (11). Those are

$$v_{p0}=\frac{\bar{k}\,\Delta H}{d_0}\times P_0;\ P_0=\frac{1}{\pi\cosh\psi_0}. \quad \cdots\cdots(12)$$

and

$$v_{pp}=\frac{\bar{k}\,\Delta H}{d_0}\times P_p;\ P_p=\frac{1}{\pi\sinh\psi_0}, \quad \cdots\cdots(13)$$

P_0 and P_p being the velocity coefficients in the seeping-in and -out points at the foundation surface and at the point just under the coffer dam, respectively, which are illustrated in Diagram 4. P_p decreases as ψ_0 increases, but the variation of P_0 is inappreciable when ψ_0 is less than about 0.2, which is resulted from the sparsity of the streamlines at the surface of the foundation, where the velocity is the lowest, far from the maximum.

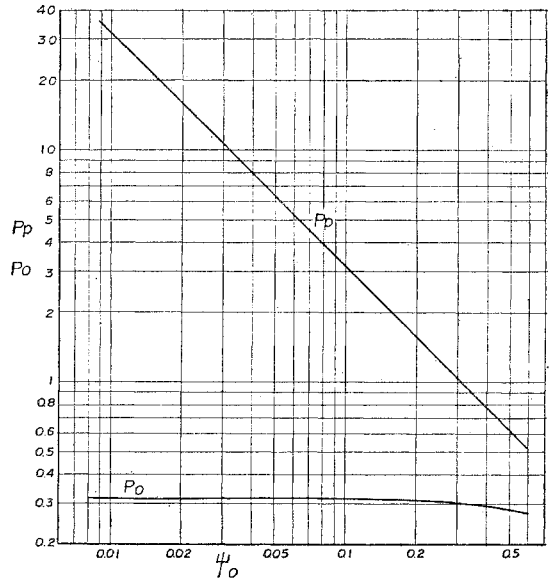

Diagram 4 P_0 and P_p-diagram.

3. Seepage velocity under a dam on an anisotropic pervious foundation of infinite thickness

Sedimentary foundation, in its natural condition, is always anisotropic in regard to permeability. The flow net of such an anisotropic foundation does not posess its usual characteristics. However, it was shown mathematically[5] that by transforming the entire cross-section in such a manner that all dimensions in the horizontal direction are reduced by the factor $\sqrt{k_v/k_h}=1/\lambda$, the problem is again reduced to a solution of Laplace's equation as discussed in the previous section.

Thus, the streamline in an anisotropic foundation is represented by the following equations,

$$x-b=\pm\frac{\lambda d_0}{\sqrt{2}}\sqrt{\sqrt{(\xi^2-\eta^2-1)^2+4\xi^2\eta^2}+(\xi^2-\eta^2-1)};$$
$$y=\frac{d_0}{\sqrt{2}}\sqrt{\sqrt{(\xi^2-\eta^2-1)^2+4\xi^2\eta^2}-(\xi^2-\eta^2-1)},$$
$$\cdots\cdots(14)$$

where

$$\xi=N\xi'+M;\ \eta=N\eta';$$
$$M=\frac{1}{2}\left[\sqrt{1+\frac{\left(\frac{1}{2}-\frac{b}{w_0}\right)^2}{\lambda^2\left(\frac{d_0}{w_0}\right)^2}}-\sqrt{1+\frac{\left(\frac{1}{2}+\frac{b}{w_0}\right)^2}{\lambda^2\left(\frac{d_0}{w_0}\right)^2}}\right];$$
$$N=\frac{1}{2}\left[\sqrt{1+\frac{\left(\frac{1}{2}-\frac{b}{w_0}\right)^2}{\lambda^2\left(\frac{d_0}{w_0}\right)^2}}+\sqrt{1+\frac{\left(\frac{1}{2}+\frac{b}{w_0}\right)^2}{\lambda^2\left(\frac{d_0}{w_0}\right)^2}}\right],$$
$$\cdots\cdots(15)$$

ξ' and η' being coordinates of the point on the ellipse having the eccentricity $e=1/\cosh\psi_0$. The seepage velocity v_s at an arbitrary point along the streamline ψ_0 is given by

$$v_s=\frac{\bar{k}_\lambda \Delta H}{w_0}\times\frac{K}{L};$$
$$K=[2(1-e^2)\{(\xi^2-\eta^2-1)^2+4\xi^2\eta^2\}\{(\lambda^2+1)\times\sqrt{(\xi^2-\eta^2-1)^2+4\xi^2\eta^2}+(\lambda^2-1)(\xi^2-\eta^2-1)\}]^{1/2};$$
$$L=\frac{\pi}{\frac{d_0}{w_0}}\sqrt{Q}$$
$$Q=[2\lambda\{\eta^2(\xi^2+\eta^2+1)+(1-e^2)\xi(\xi-M)\times(\xi^2+\eta^2-1)\}]^2+\eta^2[(\lambda^2+1)\{\xi(\xi^2+\eta^2-1)-(1-e^2)(\xi-M)(\xi^2+\eta^2+1)\}+(\lambda^2-1)\times\{\xi+(1-e^2)(\xi-M)\}\sqrt{(\xi^2-\eta^2-1)^2+4\xi^2\eta^2}]^2$$
$$\bar{k}_\lambda=\sqrt{\bar{k}_h\cdot\bar{k}_v}=\lambda\bar{k}_v,$$
$$\cdots\cdots(16)$$

$D_{0,\lambda}$, which is D_0 in anisotropic foundation, is illustrated in Diagram 5 for $\lambda=2$ and in Diagram 6 for $\lambda=4$, and $D_{p,\lambda}$, in Diagram 7 for $\lambda=2$ and in Diagram 8 for $\lambda=4$. These diagrams show $D_{0,\lambda}$ or $D_{p,\lambda}$ when a sheet pile is at the heel.

The effects of anisotropy to v_{s0} and v_{sp} are shown in Figs. 6 and 7, respectively, which show that, as the piling depth decreases, v_{s0} tends to λ^2 times and v_{sp} to λ times as large as the one in an isotropic foundation, and that, as the piling depth increases, v_{s0} tends to λ times and v_{sp} to 1 time as large.

4. Discussion on the creep theory

When sheet piling is in a single, line so-called "creep ratios" in the creep theory are represented by

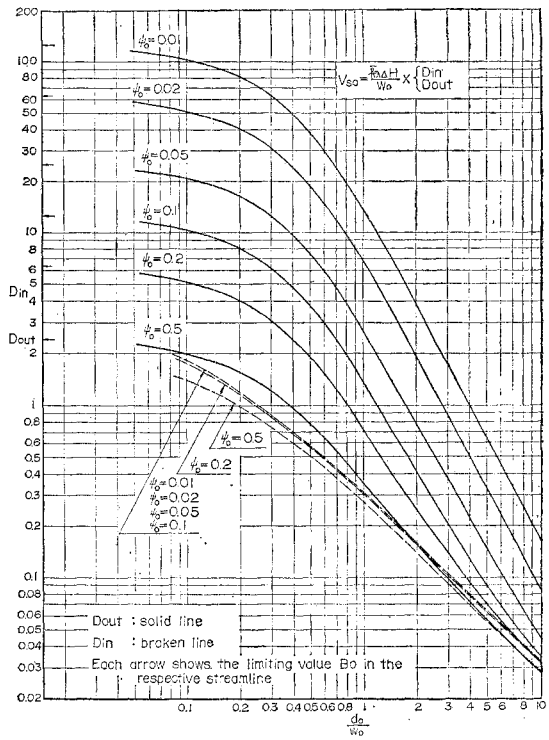

Diagram 5 $D_{0,\lambda}$-diagram ($\lambda=2$, $b=-c$ or c).

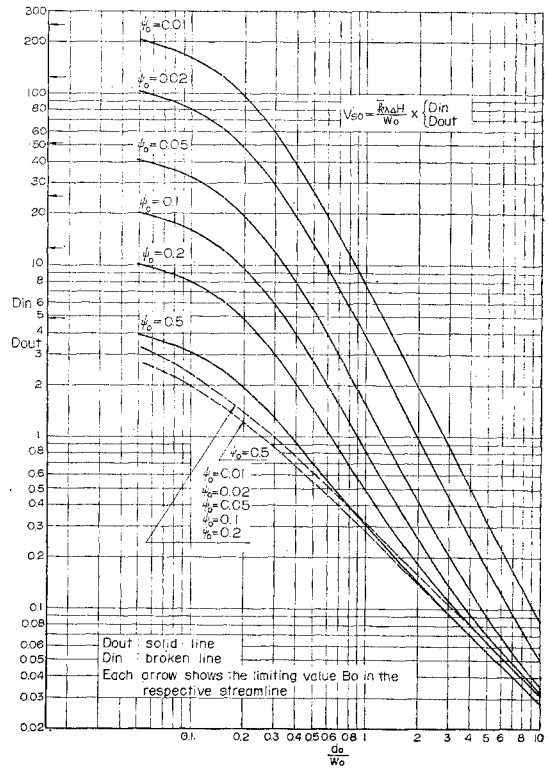

Diagram 6 $D_{0,\lambda}$-diagram ($\lambda=4$, $b=-c$ or c).

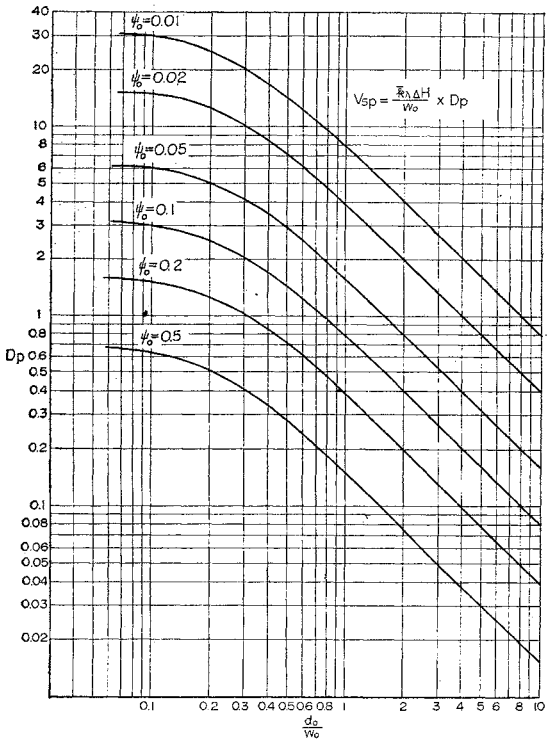

Diagram 7 $D_{p,\lambda}$-diagram ($\lambda=2$, $b=-c$ or c).

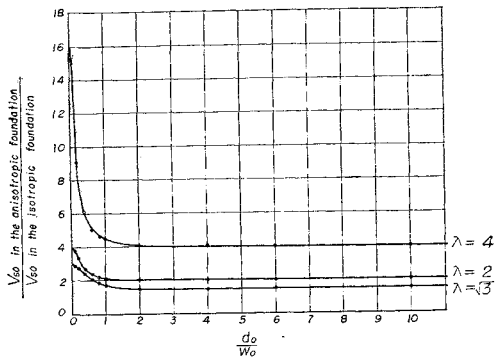

Fig. 6 Effect of foundation anisotropy to seeping-in and-out velocity v_{s0}.

$$C_c=\frac{L_c}{\Delta H}=\frac{w_0+2d_0}{\Delta H} \quad \text{and} \quad C_w=\frac{L_w}{\Delta H}=\frac{\frac{w_0}{3}+2d_0}{\Delta H}$$

where C_w may correspond to the simple creep ratio in the case of $\lambda=\sqrt{3}$, while C_c in the one in an isotropic foundation. As the reciprocals of C_c in $L_c=C_c\times\Delta H$, or C_w in $L_w=C_w\times\Delta H$ represent the limited hydraulic gradient i_c, and $v_c=\bar{k}\times i_c$, the limited velocity v_c is, in terms of the creep ratio, given by

$$v_c=\frac{\bar{k}\,\Delta H}{w_0}\times S_c\,;\ S_c=\frac{1}{1+2\left(\frac{d_0}{w_0}\right)}, \quad \cdots\cdots(17)$$

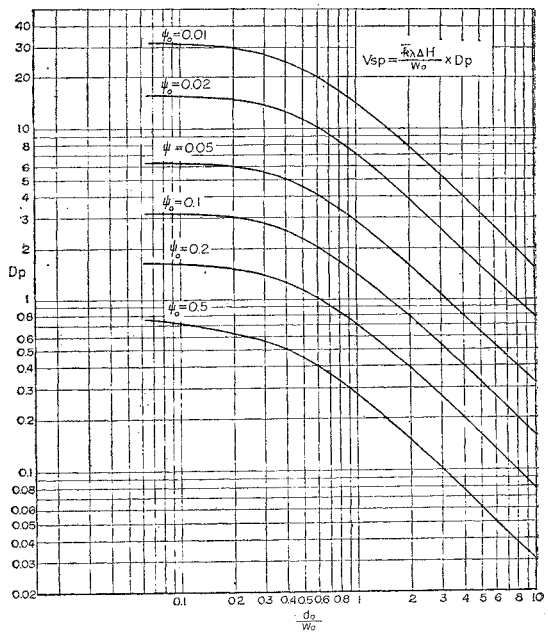

Diagrm 8 $D_{p,\lambda}$-diagram ($\lambda=4$, $b=-c$ or c).

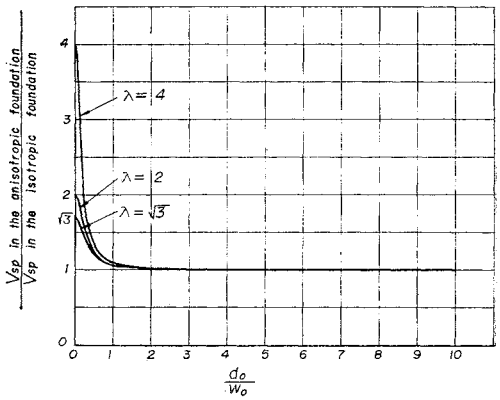

Fig. 7 Effect of foundation anisotropy to the maximum velocity v_{sp} near the extremity of sheet piling.

or

$$v_w=\frac{\bar{k}\,\Delta H}{w_0}\times S_w\,;\ S_w=\frac{1}{\frac{1}{3}+2\left(\frac{d_0}{w_0}\right)}. \quad \cdots\cdots(18)$$

Eqs. (17) and (18) are similar to Eqs. (10) and (11) in form, and S_c or S_w are dimensionless quantities, directly comparable to and with D_0 or D_p. Thus they may be called the velocity coefficient equivalent in the creep theory. The values of S_c are compared with D_0 in Diagram 2 and with D_p in Diagram 3 and the values S_w with $D_{0,\lambda=\sqrt{3}}$ in Fig. 8 and $D_{p,\lambda=\sqrt{3}}$ in Fig. 9. As readily seen in these figures, both S_c and S_w may almost correspond to D_{out} or

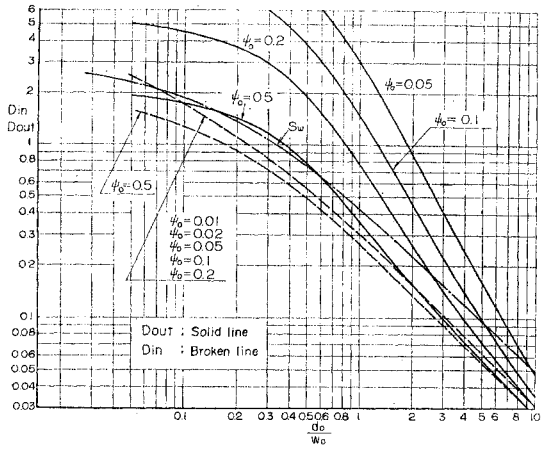

Fig. 8 Comparison of $D_{0,\lambda=\sqrt{3}}$ and S_w in the case of sheet piling at the heel or the toe of the dam.

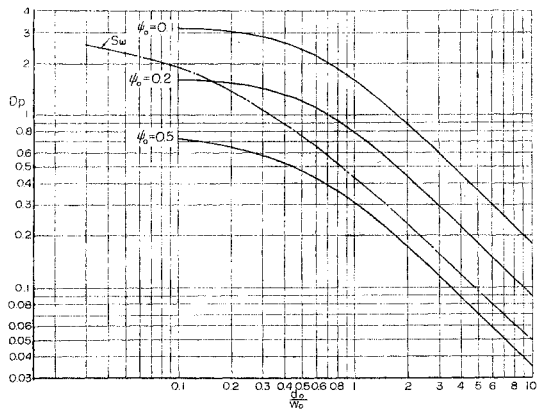

Fig. 9 Comparison of $D_{p,\lambda=\sqrt{3}}$ and S_w in the case of sheel piling at the heel or the toe of the dam.

D_p in the streamline of which ψ_0' s value is considerably large, i.e. about 0.5. In other words it will be said that the seeping-ont velocity given by the creep theory may represent the actual one at the point fairly distant from the structure, far from the one along the creep line.

Terzaghi[6] carried out the experiments to obtain the critical head differences ΔH_c when the piping phenomena broke out, both for a dam without sheet piling and for a coffer dam, each having the same creep length $2D$. It was verified from these experiments that H_c for a coffer dam of depth D was $3.0D$ and for a dam of width $2D$ without sheet pile, was $1.2D$, which was contrary to expectations that both differences must become equal if the simple creep theory held. However, the seeping-out velocity in the dam of the base width $2D$ without sheet pile is given, from Eq. (10), by $v_{s0}=\bar{k}\Delta H/D \times B_0/2$, and the one in the coffer dam of depth D is given, from Eq. (12), by $v_{s0}=\bar{k}\Delta H/D \times P_0$. Therefore, the seeping-out velocities in both cases can be compared through the comparison between B_0 and P_0. As $B_0>2P_0$ always in the streamline comparatively near the structure, the velocity in the former is much greater than in the latter, which may semi-quantitatively explain Terzaghi's experiments, though its detail cannot be known, if the break-down of the foundation in his experiments commenced from vertical piping.

5. Experimental verification

The limited hydraulic gradient $i_c=v/k$ in the vertical piping phenomenon at the discharging point is given by

$$i_c=(1-p)(\gamma-1), \quad \cdots\cdots(19)^{7)}$$

or

$$i_c=1.689-1.786\,p, \quad \cdots\cdots(20)^{8)}$$

p being the porosity of the foundation and γ, the real specific gravity of the foundation material. On the other hand, the seeping-out velocity in the streamline ψ_0 in the dam of width w_0 with sheet piling of depth d_0 is given by $v_{s0}=\bar{k}\Delta H\times(B_0$ or $D_0/w_0)$ as previously shown. Thus, the measurements of the limited water level difference ΔH_c for the various streamlines in the dam foundation will allow the relative comparisons of B_0 and D_0 and even the quantitative checks of themselves, if Darcy's formula holds until the quicksand phenomenon breaks out, through

$$i_c=\frac{\Delta H_c}{w_0}\times(B_0 \text{ or } D_0). \quad \cdots\cdots(21)$$

5.1 Arrangements for experiments

The pervious foundation 40 cm deep was formed in the water tank (120 cm×70 cm×10 cm) with medium sand (grain size=0.42 mm~0.59 mm) analysed with sieve. Plate-glass was provided in front of it as shown in Fig. 10. The head water was gently supplied from a feed-tank and the excess water was issued through syphon device. A movable sluice was equipped at the end of the downstream side, over which water flowed so as the tail water

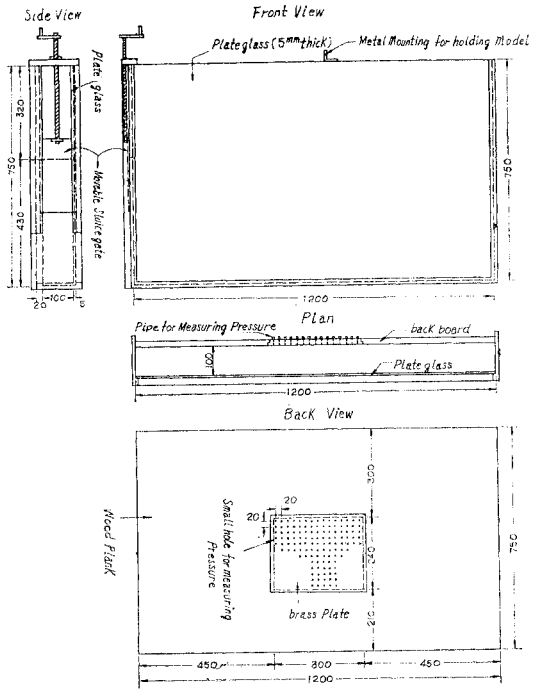

Fig. 10 Apparatus for experiment.

level was kept constant at an adequate height. In order to measure the pressure around and near the model and ensure homogeneity in the foundation, the brass plate, perforated in squares of 2 cm spacing by 120 holes 1 mm in diameter, was inserted in the back-board of the water tank, among which 50 holes were chosen according to the model configuration and connected with piezometer to show the pressure distribution in the vicinity of the model boundary. Each model was bordered by the streamline ψ_0 of the dam of width w_0, with/without sheet piling of depth d_0 at the dam center. The part of the model inserted in the foundation was made of brass, the accuracy of its boundary being within 0.1 mm. Wood block having the same width as of each brass model was sticked to it, and thin rubber plate having the same configuration as of the whole model was pasted on both sides, and then it was jammed between the front glass and the back brass plate.

Sand, cured in water for a long time, of 500 cc. at a time was falled down uniformly through water from the height of about 15 cm, resulting in settling about 2.5 mm thick at once. The brass surface was lightly greased and the utmost care was taken for good contact between the structure and the foundation material. The real specific gravity γ of the sand was 2.82, the porosity of the foundation, 47.4%, and the permeability coefficient, 0.10 cm/sec.

The configurations of the models were chosen as follows: (1) A-2 and A-3 have the same value of $w_0/B_0=2.0$, so the same ΔH_c is expected through Eq. (21) for these two. Thus A-2 and A-3 have the configurations of the streamline depending upon $\psi_0=0.1$ and 0.2 respectively and w_0 resulting from $w_0/B_0=2.0$ and B_0's value through B_0-ψ_0 diagram. (2) A-1, A-2, and A-4 have the same width $w_0=12.72$ cm, so ΔH_c's values by experiments are expected to be, through Eq. (21), inversely proportional to their B_0's values corresponding to $\psi_0=0.2$, 0.1, and 0.05 respectively. (3) B-1, B-2, B-3, and B-4 having the sheet pile in the center were chosen under the similar procedure. These were summarized in Table 1 and illustrated in Figs. 11. A few examples are shown in Photo. 1.

Table 1 Demensions of models for experiments

(a) In the case of dam without sheet piling

Model No.	w_0 (cm)	ψ_0	B_0	w_0/B_0	w
A-1	12.72	0.2	3.18	4.0	12.98
A-2	12.72	0.1	6.36	2.0	12.78
A-3	6.36	0.2	3.18	2.0	6.55
A-4	12.72	0.05	12.72	1.0	12.74

(b) In the case of dam with sheet piling

Model No.	w_0 (cm)	d_0 (cm)	d_0/w_0	ψ_0	D_0	w_0/D_0	w	d
B-1	8.00	9.28	1.16	0.2	0.54	14.8	8.98	9.50
B-2	8.00	9.28	1.16	0.05	2.0	4.0	8.06	9.29
B-3	8.00	3.12	0.39	0.2	2.0	4.0	8.26	3.28
B-4	8.00	9.28	1.16	0.01	9.8	0.816	8.00	9.28

Each model was slowly lowered in water and

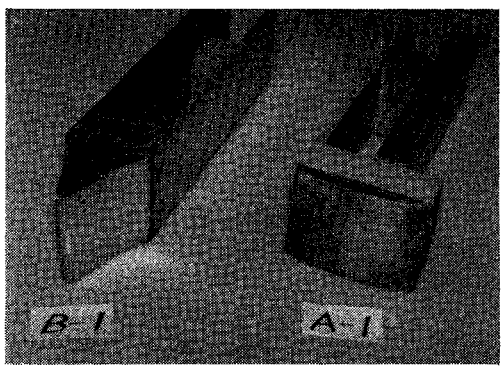

Photo 1 Examples of model.

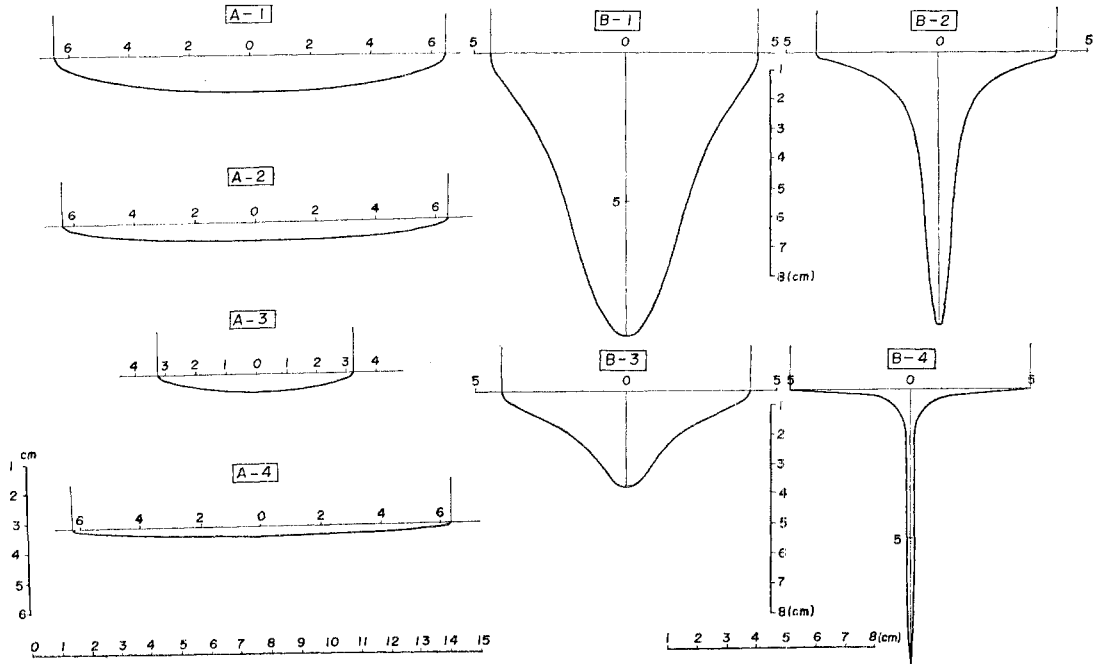

(a) a dam without sheet piling (b) a dam with sheel piling

Fig. 11 Configurations of models for experiments.

fixed at the preassigned position for the measurement of the pressure around the model, and then the sand was uniformly packed to form the pervious foundation with great care. Then, the tail water level was gently lowered until ΔH became to some centimeters, and the pressure distribution around the model was measured. Until its distribution was consistent with the calculated one, the formation of the sand layer, the insertion of the model and the enough contact of the model with the foundation were repeated. After the consistency was ascertained, ΔH was gently enlarged, and the critical difference ΔH_c when quicksand phenomenon commenced to occur was measured. Once the phenomenon occured, the head water was lowered until it ceased, and the measurement was repeated to ensure the reliability of ΔH_c's value. The occurence of quicksand phenomenon was easily observed with the naked eye through the front glass under an adequate illumination. These are shown in Photos. 2 (a) & (b).

As the sand grain size was confined within relatively narrow range, the observed phenomenon is considered to be the representative one. And, as the largest width of dam was 12.98 cm, and the largest depth of sheet pile, 9.43 cm, as compared with the thickness of the sand

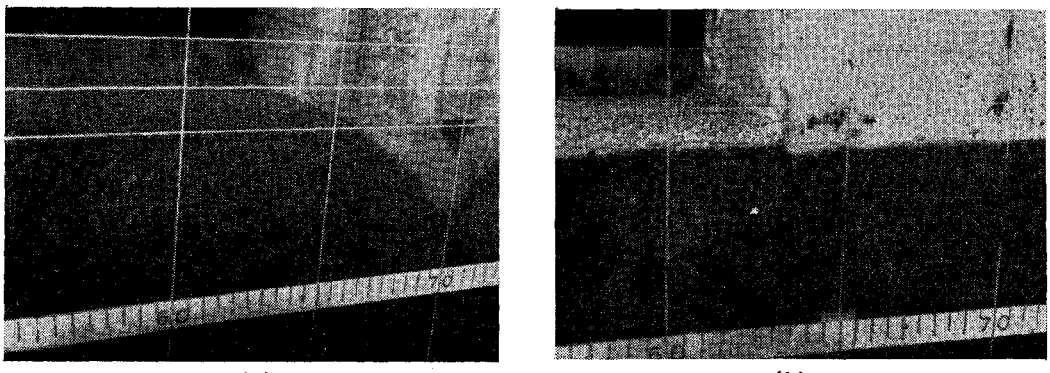

(a) (b)

Photo 2 Occurence of quick-sand phenomena.

layer, 40 cm, the pressure distribution and the seepage velocity was considered to be almost the same as in the case of the foundation having infinite depth.

5.2 Results of the experiments and consideration

Each experimental value of ΔH_c was evaluated by averaging the values obtained in more than 10 trials. As any other factors might have some influences near the contact portion of the model with the front/rear glass, ΔH_c's values near that portion were rejected on averaging.

ΔH_c can be evaluated theoretically by Eq. (21) if only i_c, w_0, and B_0 or D_0 are given, and the ratio of ΔH_c in each case may represent the corresponding ratio of velocity coefficients, canceling other factors concerning the foundation.

Table 2 Results of experiments

Model No.	ψ_0	w_0 (cm)	B_0 or D_0	ΔH_c (cm) (A) calc.	ΔH_c (cm) (B). obs.	(B)/(A)	$\frac{(\Delta H_c)}{(\Delta H_c \text{ in B-1})}$ (C) calc.	(D) obs.	(D)/(C)
A-1	0.2	12.72	3.18	3.84	4.9±0.07	1.28	27.0	29.0	1.07
A-2	0.1	12.72	6.36	1.92	2.7±0.13	1.41	13.5	16.0	1.18
A-3	0.2	6.36	3.18	1.92	2.7±0.05	1.41	13.5	16.0	1.18
A-4	0.05	12.72	12.72	0.96	1.6±0.05	1.67	6.8	9.6	1.41
B-1	0.2	8.00	0.54	14.20	16.9±0.29	1.19	100.0	100.0	1.00
B-2	0.05	8.00	2.0	3.84	4.3±0.08	1.12	27.0	25.4	0.94
B-3	0.2	8.00	2.0	3.84	4.3±0.12	1.12	27.0	25.4	0.94
B-4	0.01	8.00	9.8	0.78	5.6±0.33	7.18	5.5	33.1	6.0

Table 2 shows these comparisons in each case, and Fig. 12 illustrates an example of the comparison of the observed pressure distribution with the calculated one.

Meanwhile, the seepage flow characteristics

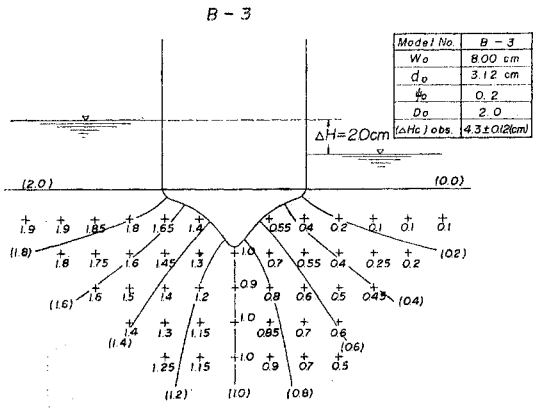

Each figure shows observed pressure at + point, solid line shows theoretical equipressure curve and the figure in each branket is its value.

Fig. 12 An example of pressure distribution in the experiment.

Table 3 Reynolds number in each model in the experiment

Model No.	w_0 (cm)	(ΔH_c)obs. (cm)	B_0 or D_0	v_0 (cm/sec)	R_0	D_p	v_p (cm/sec)	R_p
A-1	12.72	4.9	3.18	0.12	0.52	—	—	—
A-2	12.72	2.7	6.36	0.14	0.57	—	—	—
A-3	6.36	2.7	3.18	0.14	0.57	—	—	—
A-4	12.72	1.6	12.72	0.16	0.67	—	—	—
B-1	8.00	16.9	0.54	0.11	0.48	1.13	0.24	1.01
B-2	8.00	4.3	2.0	0.11	0.45	4.5	0.24	1.02
B-3	8.00	4.3	2.0	0.11	0.45	1.60	0.088	0.37
B-4	8.00	5.6	9.8	0.69	2.91	22.9	1.6	6.73

v_0 and v_p represents the maximum velocity at the seeping-in and -out points, and at the extremity of sheet piling, respectively.

R_0 and R_p represent Reynolds number at those points respectively.

should be checked by Reynolds number. Table 3 shows those numbers at the maximum velocity points in all cases at the critical head differences, the mean diameter of grains being 0.505 mm, the specific gravity of water, 1, its viscosity in 13°C at the time of measurement, 0.012 poise. As shown in Table 3, Reynolds number in every case except in B-4 becomes to about or less than 1. Consequently, it may be concluded that all experiments except in B-4 were under the laminar flow, which was a presupposition in this treatment.

It may be found that the comparison of the observed value of ΔH_c with the calculated one in Table 3 shows the comparatively good agreement in both its absolute and relative values in all cases except in B-4, whether there is sheet piling or not. The fact that the deviations in $(D)/(C)$ is less than in $(B)/(A)$ will be due to canceling possible errors in the measurements of the specific gravity of sand or, especially, the porosity of the foundation and others, for estimating i_c, and the deviation in $(D)/(C)$ will contain the error accompanied by the technical difficulty of the close contact of the model having the different configuration with the foundation having the identical porosity.

It is noted, however, that in B-4 the observed value is conspicuously different from the calculated one. The following two will be considered as the cause of such discrepancy; (1) Because of the very small streamline value in B-4, the boundary of the model is very close to the original frame especially near the maximum velocity points. Accordingly, the radii of curva-

ture at these points become too small to be made in the accuracy of 0.1 mm. And moreover, the sand grain is too large in size to examine the flow at the point having such small radius of curvature. Thus the discharging flow condition at the downstream surface might become different from the theoretical one. The similar tendency will be seen in the result in A-4, too. In real dam, however, as w_0 becomes numerically very large, the radius of curvature also becomes large for the same ψ_0's value, while the grain size for foundation remains almost as it is in the experiment. Therefore, the flow behaviour in an actual dam would tend to the theoretical one. (2) Reynolds unmbers of both R_0 and R_p in B-4 are much greater than in other cases, which shows that, when the head difference becomes ΔH_c, the flow characteristics might change to the turbulent flow around the extremity of sheet piling, and might become beyond the range of validity of Darcy's law. Therefore, result in B-4 may be found not to be under the laminar flow. It is thus considered that the difference in B-4, though it is in safe side in the actual application, will be due to the combination of them.

Thus it may be considered that the theoretical estimation of the velocity coefficients of B_0 and D_0 in an homogeneous and isotropic foundation is verified experimentally within the range of errors to some extent. It is noted that, in spite of the same length of the original frame w_0 in A-1 and A-2, slight change in the configuration by the difference of ψ_0 leads to the remarkable difference between ΔH_c for them. B-1 and B-2 are in the same case. Further, though A-2 has twice the width of A-3, these two have almost the same ΔH_c. These phenomena cannot be explained by the "creep theory," and show the variation of the seepage veloeity with the streamline under a floating dam.

The practical application of this relation would sometimes enable to design the more reasonable and economical section of a floating dam. In other words, some deformation of the dam base will enable to diminish the piling depth or the base width against scouring in a floating dam. The larger value ψ_0 has, the less the absolute value of the velocity at its maximum point becomes, and therefore, the shorter piling depth for an identical ΔH_c becomes. However, as ψ_0's value becomes large, the base form bordered by the streamline becomes more voluminous as in B-1, which will be not practical in the actual design. It is noted here that the most important is the flow condition near those points and the seepage velocity along a streamline becomes small except in the maximum points. It may be seen, therefore, that some deformation of the structure boundary in portion having such lower seepage velocity, if only doing so does not make an appreciable change in the flow condition near the essential points, becomes more practical in the application. Such deformation will make, strictly speaking, some change in the flow behaviour, but it will be expected that it will make little change in the whole system to remain the dead water zone as it is, as the seepage velocity in such portion is much lower. Thus, the similar experiments in the model of which the above-mentioned portion was cut away were tried.

5.3 Supplementary experiments for practical application

The effect of deforming the lower velocity portion of models to the limited head difference was examined, abopting A-1 and B-1 as illustrations. The deformed model of A-1 was named A-1′. B-1 was twice deformed and they were named B-1′ and B-1″, as illustrated in Fig. 13. Thus A-1′ and B-1″ will become similar to the actual floating dam with cut-offs near the heel and the toe. The example of the pressure distributions in these cases is shown in Fig. 14. The comparison of this distribution with the theoretical one of each original form showed that some difference appeared in the deformed portion but the significant difference could not be observed near essential points though the observation points were not enough in density. Table 4 showed that the observed ΔH_c in each case decreased with deformation in spite of the longer creep length. This phenomenon will be due to the fact that the pressure drop near the essential points becomes larger than in the original form, which results in increasing the hydraulic gradient. The absolute value of ΔH_c in

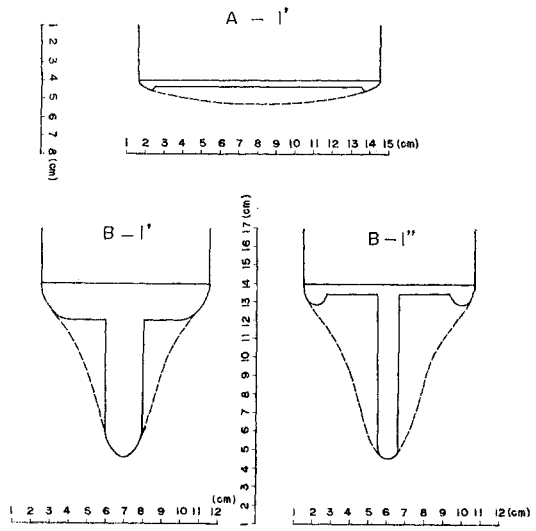

Fig. 13 Cross-sectional configurations of deformed models.

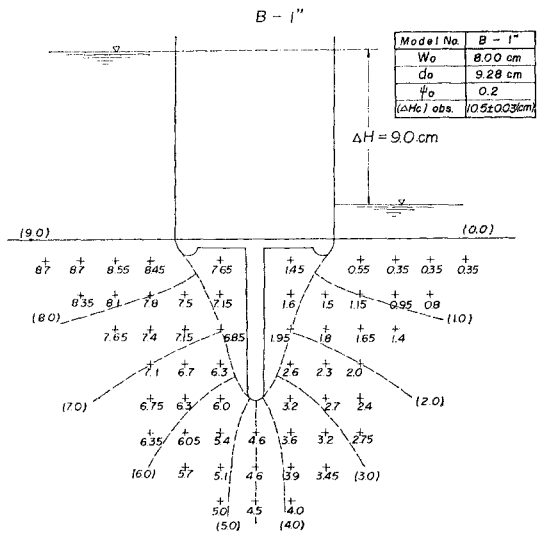

Each figure shows observed pressure at + point, solid line shows theoretical equipressure curve and the figure in each branket is its value.

Fig. 14 An example of pressure distribution in the deformed model.

A-1′ amounts to 92 % of it in A-1, and ΔH_c in B-1″, which is remarkably deformed from B-1, to about 60 % of it in the original form. That is to say, B-1″ can be still proof against about 2.4 times as high as ΔH_c in B-2, of which the basic frames w_0 and d_0 are the same as the former. The indication of the streamline in the deformed model B-1″ by the coloured liquid shows to be similar to the original

Table 4 Results of experiments in the deformed models

Model No.	w (cm)	d (cm)	(ΔH_c) obs in the deformed (A)	in the original (B)	(A)/(B)
A-1′	12.98	—	4.5±0.08	4.9±0.07	0.92
B-1′	8.98	9.50	14.0±0.09	16.9±0.29	0.83
B-1″	8.98	9.50	10.5±0.30	16.9±0.29	0.62

boundary, and that the cut away portion may become to the dead water zone or the like, as in Photo. 3. Further, it may be concluded from these experiments that cut-offs in the actual dam are much effective to its safety and moreover cut-offs with an adequate configuration will enable to decrease the necessary dimensions of sheet pile and dam itself.

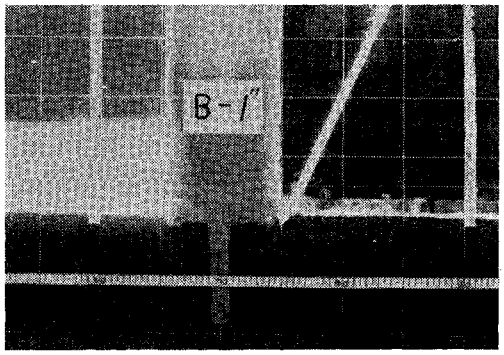

Photo 3 Indication of streamline by coloured fluid.

6. Application to the security analysis of a floating dam from underseepage

The seepage velocity under a floating dam becomes maximum in 3 points as described in the preceding section. So, if the velocities in these points do not exceed a certain limited value, the dam would be secured from under seepage. Among these points, seeping-out point from the foundation is clearly more dangerous in scouring than seeping-in point in general, and the scouring at the former is the so-called vertical piping. The limited hydraulic gradient i_c for it is given by Eq. (19) or Eq. (20). While, scouring near the extremity of sheet pile is different in its mechanism from vertical piping and called the subsurface erosion. Though the limited velocity against it is not yet theoretically analysed, a certain value v_c should exist against a kind of foundation material, such as the permissible velocity advocated by J.D. Justin[9].

From these i_c and v_c, a floating dam secured

from underseepage may be generally analysed as follows : (1) The foundation properties (effective permeability, porosity, size and specific gravity of materials etc.) at a dam site and the basic dam width w_0 necessary for the stabilization of itself are first to be known. (2) As the velocity at the seeping-out point is given by $v_{s0} = (\bar{k}\,\Delta H/w_0) \times D_0$, the hydraulic gradient i at its point becomes $i = (v_{s0}/\bar{k}) = (\Delta H/w_0) \times D_0$. As $i_c > i$ should prevent from vertical piping, $D_0 < i_c \times w_0/\Delta H$ must be satisfied. Here, as i_c, w_0, and ΔH are all given quantities, the maximum value of D_0 can be evaluated. From the corresponding diagram of D_0 depending upon the position of sheet pile and anisotropy in the foundation, values of d_0/w_0 can be estimated for various ψ_0's values. (3) Next, as D_p's value can be read from D_p diagram corresponding to the above d_0/w_0, ψ_0, the position of sheet piling, and anisotropy of the foundation, and thus the seepage velocity v_{sp} around the extremity of sheet pile is estimated through $v_{sp} = (\bar{k}\,\Delta H/w_0) \times D_p$. As v_{sp} must be less than v_c in order to prevent from subsurface erosion, $v_{sp} < v_c$ will fix the limits of the above $(d_0/w_0) - \psi_0$ relation, which secures from all scouring, and leads to calculate the streamline. Here, $\bar{k} = k_a$ (macroscopic velocity) $\times \tau/p$, τ being the foundation tortuosity (generally 1.3~1.7), and p, the porosity. Thus, the base configuration being chosen along one of the above obtained streamlines, it will give a floating dam secured from all scouring by underseepage. The actual configuration must be singled out of the various streamlines from the economical and technical view points.

But, as the base structure becomes voluminous with increase of ψ_0, such configuration will sometimes become impracticable. In such a case, some portions inessential to the scouring could be saved by the appication of the supplementary experiment described in 4.3. However, it is necessary in this case that D_0 should be multiplied, in anticipation, by a certain factor as the deformation leads to enlarge the seepage velocity in essential points, and moreover that the velocity coefficient in the deformed model should be confirmed by comparison with the original one by the model experiments. In all cases, great care should be taken in the close contact of the structure with the foundation.

The above method would be applied not only to the so-called floating dam but also to the treatment of the fault or fractured zone which a dam rests on and intersects to its axis, or to the necessary depth of curtain grouting, if the foundation in these eases are regarded as a porous medium and the seepage flow system holds Darcy's formula.

7. Conclusion

The seepage flow velocity under a dam resting on a homogeneous foundation of infinite thickness, either isotropic or anisotropic, were theoretically analysed under the presupposition that the flow holds Darcy's formula. It was found that the seepage velocity becomes maximum in the seeping-in and -out points at the foundation surface and near the extremity of sheet pile. Thus the velocity coefficients were defined and evaluated in diagrams, with which the seepage velocities at its maximum points, essential in designing a safe floating dam, could be easily estimated for an arbitrary dam width, sheet piling depth and water head. The influence of the dam width, the position and the depth of sheet piling, and anisotropy in the foundation to the seepage velocity were discussed. It was found that cut-offs at heel or toe were very effective to diminish the seepage velocity at its maximum point. The so-called "creep theory" was quantitatively criticized and it was shown that the velocity by the theory is numerically only the maximum velocity at comparatively distant point from the structure. The velocity coefficients obtained theoretically were confirmed experimentally, and the more reasonable method than before of analysis of a floating dam secured from underseepage was developed.

Finally, the author wishes to express his hearty gratitude to Dr. M. Homma, Professor of Tokyo University, and Dr. S. Shima, Assistant Professor of Tokyo University, who gave him many suggestions and guidances, and to tender his many thanks to Dr. H. Tanaka and others, staffs of Geological Section, Central Research Institute of Electric Power Industry, who gave him many advices and encouragements.

Reference

1) Lane, E.W. : "Security from underseepage masonry dams on earth foundations", A.S.C.E., Trans., Vol. 100 (1935), pp. 1235-1272.
2) Awazu, S. : "Fundamental research on the scouring mechanics", Trans., fo J.S.C.E., No. 52, 1958, pp. 1-25.
3) Yahagi, F. : "Studies on the underseepage velocity in the dam on the pervious foundation" (in Japanese), Tech. Rept., C.R.I.E.P.I., C 60011, 1961.
4) Muskat, M. : "The flow of homogeneous fluids through porous media", McGraw-Hill Co. (1946) p. 181.
5) Schaffernak, F. : "Erforschung der physikalischen Gesetze, nach welchen die Durchsickerung des Wassers durch eine Talsperre oder durch den Untergrund stattfindet", Die Wasserwirtschaft, (1933), No. 30.
6) Terzaghi, K. : "Effect of minor geologic details on the safety of dams", Bull. A.I.A.E., Tech. Pub., 215 (1929) Class 1, Mining Geology, No. 26, pp. 31-46.
7) Terzaghi, K. : "Der Grundbruch an Stauwerken und seine Verhüttung", Die Wasserkraft, 1922.
8) Awazu, S. : "Few properties of bed material and its application", Trans., of J.S.C.E., No. 36,1956, pp. 30-37.
9) Justin, J.D. : "The design of earth dams", A.S.C.E., Trans., Vol. 87, (1924) p. 49.

昭和 37 年 7 月 15 日印刷
昭和 37 年 7 月 20 日発行

土木学会論文集 第 83 号

定価 150 円 (〒 20 円)

編集兼発行者 東京都新宿区四谷一丁目 社団法人 土木学会 末森猛雄
印刷者 東京都港区赤坂溜池 5 株式会社 技報堂 大沼正吉

発行所 社団法人 土木学会 振替東京 16828 番
東京都新宿郵便局区内 新宿区四谷一丁目 電話 (351) 代表 5138 番

昭和三十七年五月二十八日第三種郵便物認可
昭和三十七年七月十五日印刷
昭和三十七年七月二十日発行（毎月一回二十日発行）

本学会論文集第八十三号

定価百五十円